Induction of angiogenesis in tissue-engineered scaffolds designed for bone repair: A combined gene therapy–cell transplantation approach

Ehsan Jabbarzadeh*, Trevor Starnes*, Yusuf M. Khan*†, Tao Jiang‡, Anthony J. Wirtel†, Meng Deng‡, Qing Lv‡, Lakshmi S. Nair*, Steven B. Doty§, and Cato T. Laurencin*†‡¶

Departments of *Orthopaedic Surgery and ‡Chemical Engineering, University of Virginia, Charlottesville, VA 22908; †Department of Biomedical Engineering, University of Virginia, Charlottesville, VA 22904; and §Hospital for Special Surgery, New York, NY 10021

Edited by Robert Langer, Massachusetts Institute of Technology, Cambridge, MA, and approved May 21, 2008 (received for review January 3, 2008)

One of the fundamental principles underlying tissue engineering approaches is that newly formed tissue must maintain sufficient vascularization to support its growth. Efforts to induce vascular growth into tissue-engineered scaffolds have recently been dedicated to developing novel strategies to deliver specific biological factors that direct the recruitment of endothelial cell (EC) progenitors and their differentiation. The challenge, however, lies in orchestration of the cells, appropriate biological factors, and optimal factor doses. This study reports an approach as a step forward to resolving this dilemma by combining an *ex vivo* gene transfer strategy and EC transplantation. The utility of this approach was evaluated by using 3D poly(lactide-co-glycolide) (PLAGA) sintered microsphere scaffolds for bone tissue engineering applications. Our goal was achieved by isolation and transfection of adipose-derived stromal cells (ADSCs) with adenovirus encoding the cDNA of VEGF. We demonstrated that the combination of VEGF releasing ADSCs and ECs results in marked vascular growth within PLAGA scaffolds. We thereby delineate the potential of ADSCs to promote vascular growth into biomaterials.

biomaterials | tissue engineering | VEGF | adipose derived stem cells | sintered microsphere matrix

Bone defects and non-unions caused by trauma, tumor resection, pathological degeneration, or congenital deformity have been traditionally repaired by using autografts and allografts. Because of their osteoconductivity, osteoinductivity, and osteogenicity, autografts set the gold standard for clinical bone repair (1). Nevertheless, the application of autografts is restricted because of donor shortage and donor-site morbidity. The application of allografts is also limited by the risk of disease transfer and immune rejection (2).

To overcome these limitations, tissue engineering has evolved as a means to develop viable bone grafts. In this approach, the neotissue can be constructed by using a combination of specific cells, growth factors, and 3D porous scaffolds alone or in combination (3). The success of tissue engineering strategies, however, critically depends on the extent of blood vessel infiltration into the scaffolds (4). The primary function of vasculature is to facilitate the transport of nutrients and oxygen to cells invading from the host tissue and cells transplanted in the scaffolds. Accordingly, insufficient neovascularization is demonstrated to result in the formation of fibrous capsule surrounding implants and prevention of biochemical transport into their interior (5, 6). Despite its critical role, blood vessel invasion from the host tissue is limited to a depth of several hundred micrometers from the surface of the implant (7, 8).

To promote biomaterial vascularization, a number of strategies have been developed by using (*i*) growth factors that induce endothelial cell (EC) migration and proliferation (9–11) and (*ii*) ECs or stem cells that can differentiate toward the endothelial lineage (12, 13). Both of these approaches, alone or in combination, have resulted in a significant improvement of vascular ingrowth, proving the hypothesis that the delivery of angiogenic growth factors can trigger the migration of host ECs, which potentially can graft with the ECs cultured in the scaffolds before implantation. There remain, however, three major challenges in factor delivery: (*i*) the sensitivity of growth factors to thermal processing and exposure to chemical solvents, (*ii*) the short half-life of growth factors *in vivo* (14), and (*iii*) the limited control over the spatial and temporal distribution of growth factors throughout the scaffolds.

Increasingly recognized as an alternative strategy, gene therapy has shown a significant potential to circumvent the limitations associated with conventional protein delivery strategies. Gene therapy uses genetically modified cells to deliver a bioactive protein at physiologic doses for a sustained period. Specific genes can be transferred to the cells in the patient's body (*in vivo* gene therapy). However, this approach is uncommon because of (*i*) the difficulties in targeting specific host cells and (*ii*) the risk of vector introduction into the patient. In the *ex vivo* gene therapy approaches, cells are harvested, expanded, genetically modified by using a vector (e.g., a virus), and implanted at a specific site *in vivo* (15, 16).

The development of *ex vivo* gene therapy approaches for growth factor delivery in combination with tissue engineering has opened up new avenues for treatment of various diseases. An example is the treatment of bone, in which *in vivo* implantation of biodegradable scaffolds containing adenovirus-transfected stem cells (e.g., mesenchymal stem cells) secreting osteoinductive factors demonstrated accelerated osseous neogenesis in animal models (17, 18). Another example is the development of vascular grafts for cardiovascular applications, in which viral gene therapy was used to induce overproduction of anticoagulant proteins to prevent thrombosis and enhance vascular integration with native arteries (19, 20).

Gene therapy has also demonstrated a significant promise in improvement of biomaterial vascularization through transplantation of genetically engineered cells imparting the natural secretion of angiogenic factors (21, 22). Such approaches have commonly used autologous bone marrow mesenchymal stem cells (BMSCs) for gene delivery. Under appropriate conditions, BMSCs can differentiate along osteogenic, adipogenic, myogenic, and chondrogenic lineages (23). Nevertheless, limitations on cell harvest techniques and low stem cell yield of bone marrow aspirates prompt the need for alternative sources.

It was recently discovered that adipose-derived stromal cell (ADSC) populations contain mesenchymal stem cells (24). In contrast to BMSCs, ADSCs are available in large numbers, are easily accessible, and expand rapidly *in vitro*, presenting them as an attractive cell source for tissue engineering applications (25). Subsequently, several studies showed the potency of adipose-derived

Author contributions: E.J. and C.T.L. designed research; E.J., T.S., Y.M.K., T.J., A.J.W., M.D., Q.L., and L.S.N. performed research; S.B.D. contributed new reagents/analytic tools; E.J. and C.T.L. analyzed data; and E.J. and C.T.L. wrote the paper.

The authors declare no conflict of interest.

This article is a PNAS Direct Submission.

¶To whom correspondence should be addressed at: Department of Orthopaedic Surgery, University of Virginia, 400 Ray C. Hunt Drive, Suite 330, Charlottesville, VA 22903. E-mail: laurencin@virginia.edu.

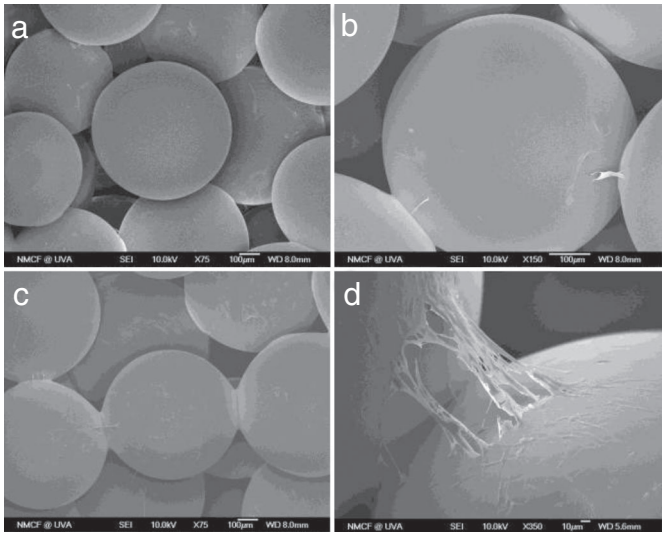

Fig. 1. Scanning electron micrographs showing ADSC proliferation at days 7 and 14 on PLAGA sintered microsphere scaffolds. (*a*) Day 7. (Magnification: ×75.) (*b*) Day 7. (Magnification: ×150.) (*c*) Day 14. (Magnification: ×75.) (*d*) Day 14. (Magnification: ×350.)

stem cells to perform endothelial differentiation, release angiogenic factors such as VEGF, and influence revascularization to a similar degree to BMSCs (26–29). Interestingly, the coculture of ADSCs with ECs resulted in a significantly enhanced EC viability and formation of tube-like structures (29). These findings all together suggested that ADSCs are involved in angiogenesis and provide an excellent candidate for gene delivery approaches.

In this study, we evaluated the potential of genetically modified ADSCs combined with ECs to direct the formation of a vascular network into tissue-engineered scaffolds. For their *in vitro* compatibility with various cell types and suitable properties for bone tissue engineering (30, 31), poly(lactide-co-glycolide) (PLAGA) 3D sintered microsphere scaffolds were used. The system developed in this study, however, is versatile and has the potential to be applied for bioengineering of other tissues such as heart and kidney.

Results

***In Vitro* Evaluation of VEGF-Producing ADSCs.** Scanning electron microscopy (SEM) images of ADSCs cultured on PLAGA scaffolds were taken at day 7 (Fig. 1 *a* and *b*) and day 14 (Fig. 1 *c* and *d*). At the earlier time point, we observed ADSC adherence to the surface of microspheres while some of the cells formed cytoplasmic extensions and bridged the gaps between the microspheres (Fig. 1 *a* and *b*). At day 14, proliferation progressed to the point that cells covered the surface of microspheres. These results confirmed that PLAGA sintered microsphere scaffolds support the attachment of ADSCs.

ELISA in 2D tissue culture polystyrene (TCPS) in combination with immunofluorescent analysis on 3D scaffolds was used to examine the VEGF release by transfected ADSCs. Fig. 2*a* shows the amount of VEGF released by transfected ADSCs as a function of multiplicity of infection (MOI) at days 3, 7, and 10 on TCPS. ADSCs (MOI = 0 PFU per cell) was considered as a control. At day 3, ADSCs produced the minimum level of VEGF (0.93 ± 0.33 ng/ml), whereas the maximum VEGF release was with ADSCs transfected at MOI = 100 PFU per cell (3.78 ± 0.34 ng/ml). As we proceeded to day 7, the level of VEGF production by MOIs >10 reached a plateau. Results at day 10 exhibited a trend of VEGF production similar to that of day 3, in which ADSCs transfected at MOI = 100 PFU per cell secreted VEGF at the highest level compared with all of the groups. Based on these results, MOI = 100 was chosen as the optimal MOI for all the rest of the *in vitro* and *in vivo* studies.

The production of VEGF by transfected ADSCs on 3D PLAGA scaffolds was evaluated by using immunofluorescence microscopy. Fig. 2*b* shows the pattern of VEGF production by transfected ADSCs cells growing on the scaffolds at day 10. We found abundant

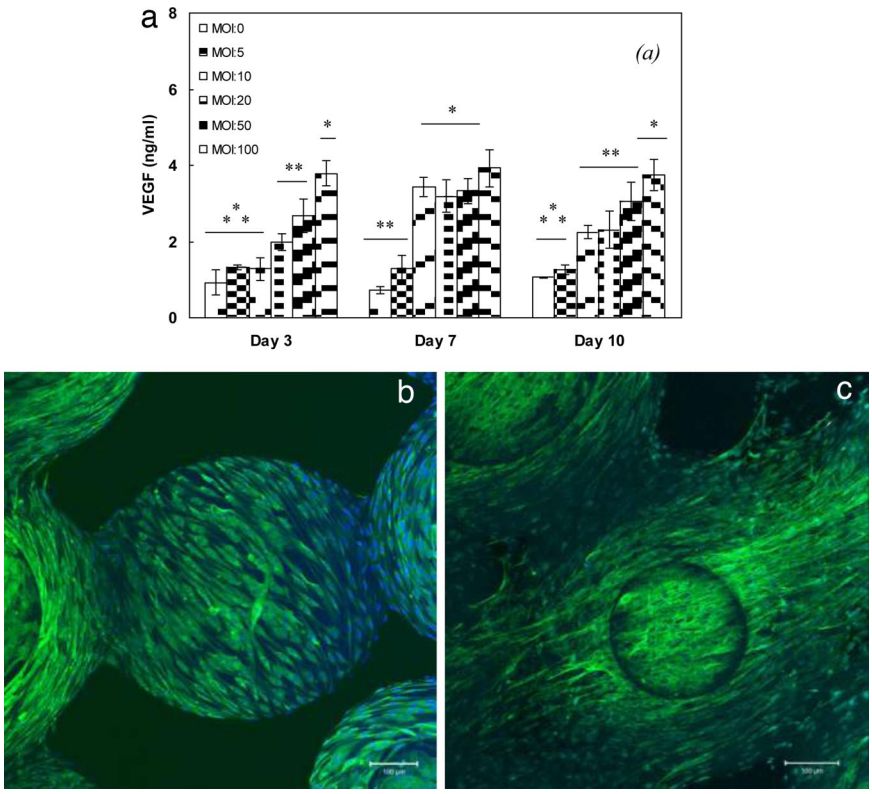

Fig. 2. VEGF production by transfected ADSCs. (*a*) The kinetics of VEGF release by ADSCs cultured on six-well plates. Data are representative of three independent experiments, and all data points are plotted as mean ± SD (n = 5). A single asterisk denotes a significantly ($P \leq 0.05$) higher VEGF production, as compared with groups denoted by two asterisks. Two asterisks denote significantly ($P \leq 0.05$) higher VEGF production, as compared with groups denoted by three asterisks. Results show that ADSCs transfected at MOI = 100 PFU per cell secreted the maximum level of VEGF as compared with other selected MOIs. The multiway ANOVA assessment did not show a significant interaction between ADSC culture time and VEGF production. (*b* and *c*) Immunofluorescent staining of VEGF production by transfected ADSCs (*b*) and nontransfected ADSCs (negative control) (*c*) cultured for 10 days on PLAGA sintered microsphere scaffolds. ADSCs were stained with antibody directed against VEGF (green) and nuclei counterstained with DAPI (blue). Images are composed of sections of the scaffolds moving through its thickness at depth increments of 4 μm and a focus depth of 224 μm that are collapsed on each other.

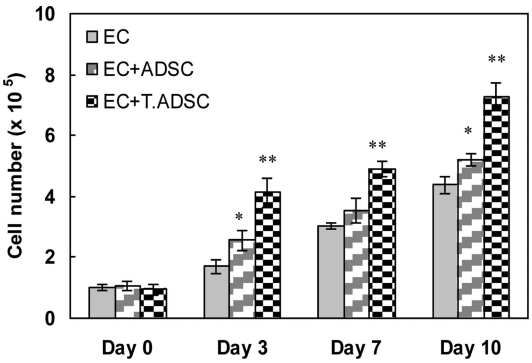

Fig. 3. EC proliferation on coculture plates containing EC alone, EC plus ADSC, and EC plus transfected ADSC. Data are representative of three independent experiments, and all data points are plotted as mean ± SD ($n = 5$). A single asterisk denotes a significantly ($P \leq 0.05$) higher EC proliferation in an EC+ADSC coculture system as compared with EC alone. Two asterisks denote a significantly ($P \leq 0.05$) higher EC proliferation in an EC+transfected ADSC coculture system as compared with EC+ADSC. The multiway ANOVA assessment did not show a significant interaction between EC proliferation and coculture time.

amounts of VEGF produced by cells on scaffolds (depicted as green fluorescence).

We evaluated the mitogenic effect of ADSCs and transfected ADSCs on ECs using a coculture system. Fig. 3 shows the proliferation of ECs at days 0, 3, 7, and 10 in three systems: (*i*) ECs alone, (*ii*) ECs plus ADSC, and (*iii*) ECs plus transfected ADSCs. Results showed that ECs proliferated at the highest rate when cocultured with transfected ADSCs. In addition, we observed a higher EC proliferation when cultured with ADSCs, as compared with ECs alone. It has been shown that ADSCs release angiogenic growth factors capable of inducing EC proliferation and differentiation (29). Among the angiogenic factors, VEGF is shown to be the most potent in enhancing the proliferation of ECs (32). We attribute the difference in proliferation of ECs to the difference in the amount of angiogenic factors (only VEGF was evaluated in this study; Fig. 2*a*) released by ADSCs in the culture medium. As shown in VEGF quantification results, transfected ADSCs released approximately four times more VEGF than ADSCs. This difference resulted in ≈145% and 60% higher proliferation of ECs at days 3 and 10 respectively, when cocultured with transfected ADSCs as compared with ADSCs. Similarly, the production of VEGF (Fig. 2*a*) and other angiogenic growth factors by ADSCs was the reason for higher EC proliferation in the coculture system with ADSCs as compared with ECs alone. These results together confirmed the mitogenic effect of ADSCs on ECs and the bioactivity of VEGF released by both transfected ADSCs and ADSCs.

***In Vivo* Evaluation.** The potential of transfected ADSCs combined with ECs to direct blood vessel growth into 3D scaffolds was evaluated by using SEM and histological techniques. The following six experimental groups were studied: (*i*) PLAGA scaffold (negative control) (blank), (*ii*) scaffold plus ECs (EC), (*iii*) scaffold plus ADSCs (ADSC), (*iv*) scaffold plus ADSCs and ECs (ADSC+EC), (*v*) scaffold plus transfected ADSCs (T ADSC), and (*vi*) scaffold plus transfected ADSCs and ECs (T ADSC+EC). At days 7, 14, and 21 after implantation, scaffolds were retrieved and assessed for the degree of vessel ingrowth. Thin sections (5 μm) were obtained from the middle of the scaffolds after which they were stained with H&E. Blood vessels were identified by the presence of red blood cells contained by a layer of ECs. Fig. 4 shows four representative images of stained sections of scaffolds containing transfected ADSCs (Fig. 4 *a* and *b*), ADSCs (Fig. 4*c*), and ECs (Fig. 4*d*) 21 days after implantation. Most of the blood vessels penetrating the

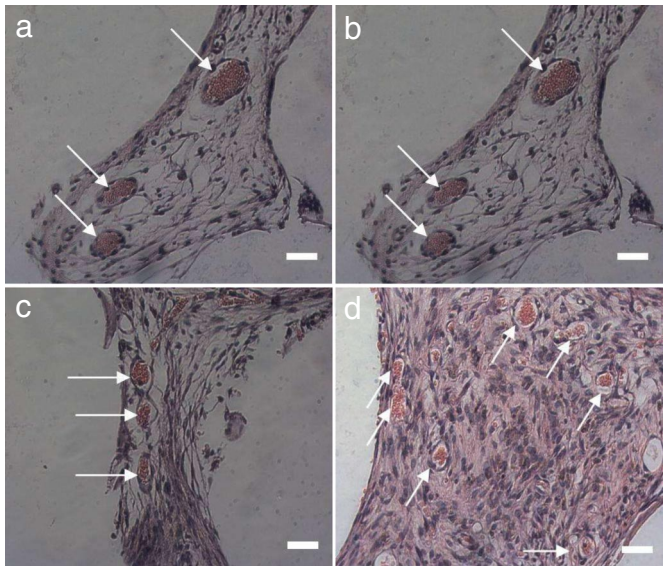

Fig. 4. Representative histological cross sections of tissue implanted with sintered microsphere scaffolds 21 days after s.c. implantation in SCID mice. (*a*) Transfected ADSCs. (Scale bar: 100 μm. Magnification: ×10.) (*b*) Transfected ADSCs. (Scale bar: 10 μm. Magnification ×100.) (*c*) ADSCs. (Scale bar: 10 μm. Magnification: ×100.) (*d*) ECs. (Scale bar: 10 μm. Magnification: ×100.) Blood vessels were identified by the presence of luminal structure containing red blood cells.

scaffolds appeared to be round. The ECs lining the blood vessels formed a consistent layer that surrounded the red blood cells.

The presence and orientation of the microvasculature within the scaffolds (2-mm depth) was also assessed by using SEM images at different magnifications (Fig. 5). Images revealed the development of blood vessels with the diameter of ≈10–20 μm lying on the surface of microspheres and bridging the gaps. Although the surface of microspheres was covered with the invading tissue, SEM micrographs showed that the pore space of the scaffolds was not fully filled by the newly formed tissue at 21 days after implantation.

The blood vessel density in scaffolds was quantified by using histological sections obtained from the middle of the scaffolds and stained with H&E. Our goal was to evaluate the combined strategy of gene therapy–cell transplantation for angiogenesis induction in PLAGA sintered microsphere scaffolds. Fig. 6 shows the density of blood vessels (number of vessels per scaffold) as a function of time. The density of blood vessels in scaffolds increased with time for all of the groups. The presence of ECs on the scaffolds resulted in an ≈46% increase in blood vessel density at 21 days after implantation as compared with blank scaffolds. Scaffolds containing ADSCs also showed a higher vessel density at days 14 and 21 than blank scaffolds. The combination of ECs and ADSCs, however, did not induce a potentiated effect.

The release of VEGF and other angiogenic factors (data not shown in this study) by transfected ADSCs led to enhanced vascular growth as revealed by the higher blood vessel density than the blank scaffolds and scaffolds seeded with ADSCs or ECs. The maximum vessel density was, however, observed in the scaffolds seeded with transfected ADSCs and ECs demonstrating a 4-fold increase compared with blank scaffolds. Results also revealed a potentiated effect of ECs and VEGF releasing transfected ADSCs by showing a higher vessel density than scaffolds seeded with either transfected ADSCs or ECs alone.

Discussion

This study involved the design of a strategy for enhancing the vascular infiltration in 3D porous scaffolds. With the use of an *ex*

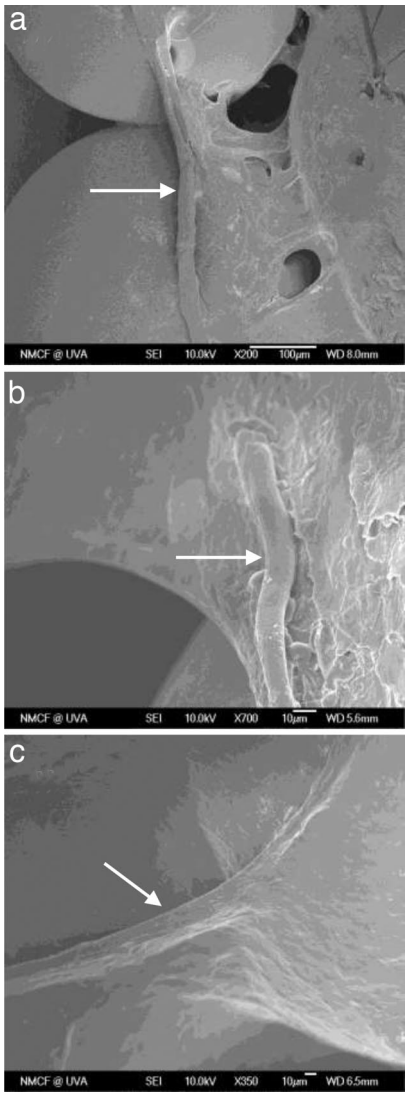

Fig. 5. SEM micrographs of blood vessel growth in the 3D PLAGA scaffolds at 21 days after implantation. [Magnification: ×200 (*a*), ×350 (*b*), and ×700 (*c*).]

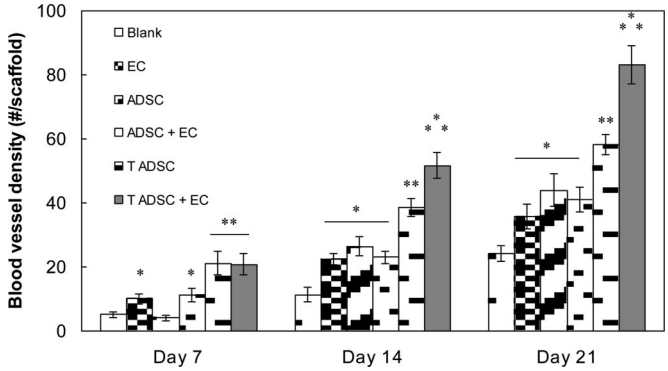

Fig. 6. Kinetics of scaffold vascularization at predetermined time points after implantation. For each group, the number of blood vessels was counted in H&E-stained slides. Each group consisted of five animals. All data points were plotted as mean ± SD. A single asterisk denotes a significantly ($P \leq 0.05$) higher number of blood vessels as compared with blank scaffolds. Two asterisks denote a significantly ($P \leq 0.05$) higher number of blood vessels as compared with scaffolds denoted by a single asterisk. Three asterisks denote a significantly ($P \leq 0.05$) higher number of blood vessels as compared with groups denoted by two asterisks. Scaffolds containing EC and transfected ADSC showed the highest number of blood vessels. The multiway ANOVA assessment did not show a significant interaction between implantation time and blood vessel density in the scaffolds.

vivo gene transfer strategy, imparting the natural release of bioactive VEGF, and EC transplantation, the formation of blood vessels through the scaffolds was significantly improved.

In the implementation of tissue engineering strategies, the choice of the donor cell type is dictated by the tissue to be repaired. In this study, ADSC was chosen because of their ability to (*i*) release angiogenic factors (28), (*ii*) enhance EC proliferation, migration, and vascular formation in coculture systems (29), and (*iii*) differentiate along endothelial lineage (27). We hypothesized that transfected ADSCs will attach and grow on the 3D PLAGA sintered microsphere scaffolds while releasing bioactive growth factors capable of inducing both endothelial growth *in vitro* and vascular ingrowth *in vivo*.

The ability of PLAGA sintered microsphere scaffolds to support the growth of ADSCs was verified by using SEM images. Results showed that ADSCs proliferated on the scaffolds and formed extensions between adjacent microspheres. This behavior was similar to the type of cellular bridging seen with other cell types in our previous studies (30, 31, 33).

Various soluble growth factors (e.g., bFGF, PDGF, and VEGF) regulate cell proliferation, migration, and cell–cell interactions during angiogenesis. Of these, VEGF is considered the most potent angiogenic growth factor that induces EC migration and proliferation. Consequently, in the treatment of ischemic tissues, VEGF has been administered either through a direct injection or with the use of delivery vehicles (34). Likewise, tissue engineering strategies have aimed to deliver VEGF in a sustained fashion to promote vascular growth in biomaterials (4). In this study, we examined the ability of Ad-VEGF transfected ADSCs to deliver bioactive VEGF on 2D TCPS and the PLAGA scaffolds. Protein quantification results demonstrated an enhanced release of VEGF by transfected ADSCs as compared with nontransfected ADSCs (MOI = 0). Whereas VEGF secretion was enhanced with higher MOIs, MOI > 100 appeared to increase cell death (data not shown). Therefore, we chose MOI = 100 as the optimal MOI for the *in vitro* and *in vivo* studies.

A drawback of viral gene therapy is the potent immune response to the virus that limits the duration of its effect. Thus, viral gene therapy approaches have mostly been studied in immune-compromised animal models. Tremendous effort has gone into characterizing the nature of immune responses to adenoviral vectors and modifying the genome of vectors to diminish the responses (35–37). In the current study we used unmodified adenoviral vectors and SCID mouse as an animal model. Our observations provide the proof of principle for the use of viral gene therapy combined with cell transplantation in treatment of disorders.

Another constraint of viral gene delivery to tissue-engineered scaffolds is the limited attachment of transfected cells to the scaffolds. In addition, adenoviral vectors transfect a cell transiently, and the production of the desired protein decreases when the cell divides (38). Therefore, practically speaking, the number of transfected cells that produce biological factors for a sustained period on the scaffolds might be limited.

In our system, the production of VEGF by ADSCs on the PLAGA scaffolds was characterized by using immunofluorescence microscopy. Results showed strong production of VEGF at both the interior and periphery of cells. It is noteworthy that in most viral gene therapy approaches, the transfection efficiency is <100%. Consequently, when cells are seeded on the scaffolds, both ADSCs and transfected ADSCs constitute the total cell seeding density. Hence, the VEGF-stained cells in immunofluorescent images in

this work include indistinguishable populations of ADSCs and transfected ADSCs.

The potential loss of bioactivity due to chemical instability issues combined with the short half-life of growth factors minimizes their therapeutic effects. Gene therapy provides a means to avoid the limitations (e.g., exposure to toxic chemicals) with traditional delivery strategies. In this study, the mitogenic effect of VEGF-secreting ADSCs was examined by using a 2D coculture model where ECs were in proximity to transfected ADSCs. Results revealed progressive proliferation of ECs when cocultured with transfected ADSCs, demonstrating the bioactivity of the secreted VEGF. It is worth noting that, in addition to VEGF, the secretion of other angiogenic factors (e.g., hepatocyte growth factor, HGF) (29) may also be involved in the mitogenic effect of ADSCs on ECs. This necessitates further studies to parse out the secretion of all of the angiogenic factors by ADSCs and assess their individual and combined effects on EC proliferation and differentiation to microvessels.

The *in vivo* data demonstrated the ability of dual transplantation of VEGF-releasing ADSCs and ECs to direct the growth of blood vessels into 3D PLAGA scaffolds. In agreement with other studies, the presence of precultured ECs on the scaffolds resulted in enhanced vascular ingrowth compared with blank scaffolds (12, 13). Further studies, however, are necessary to assess the EC differentiation into neovessels and their integration with the host vasculature.

Transplantation of ADSCs onto the PLAGA scaffolds also promoted blood vessel formation. These results were consistent with other studies showing the potential of ADSCs to improve neovascularization in ischemic limbs (26–28). The higher vascular density can be attributed to the (*i*) release of angiogenic factors by ADSCs and (*ii*) participation of the EC progenitors in ADSC populations in vascular formation. Nevertheless, a potentiated effect of combined ADSCs and ECs was not observed. In contrast, Ad-VEGF transfected ADSCs and ECs demonstrated a potentiated effect and resulted in the highest blood vessel density in scaffolds at all of the time points. We speculate that the high amounts of VEGF released by transplanted Ad-VEGF transfected ADSCs led to enhanced (*i*) proliferation of transplanted ECs, (*ii*) migration of host ECs into the scaffolds, and (*iii*) activation and differentiation of EC progenitors present at ADSC populations. Consequently, the orchestration of multiangiogenic stimulators including ECs, EC progenitors in ADSCs, VEGF, and other angiogenic factors released by ADSCs, as demonstrated by other studies (24–26), directed the formation of the blood vessel network into the PLAGA scaffolds with a 4-fold increase in vessel density compared with blank scaffolds.

It is worth noting that, in contrast to the *in vitro* coculture study, ADSCs and ECs were in physical contact in the *in vivo* study. Physical contact between different cell types may play an important role in cell differentiation and tissue developments. As an example, in a study by Kang *et al.* (39), the physical contact between ADSCs and neural stem cells was shown to be necessary for induction of neural differentiation. A study by Elbjeirami and West (40) also emphasized the role of physical contact between VEGF transfected smooth muscle cells and ECs in the formation of capillary-like structures by ECs. In this study, we anticipate that ECs cocultured in physical contact with transfected ADSCs form microvessels on the scaffolds. Nevertheless, further research is necessary to explore the interactions of ECs and ADSCs mediated by paracrine and juxtacrine cues.

The complexity of the angiogenesis process indicates the need for a combination of various cell types and growth factors in strategies for vascularization of biomaterials. The present study took a step toward this goal by combining the strategies of gene therapy and cell transplantation. This was achieved by seeding Ad-VEGF transfected ADSCs and ECs on 3D PLAGA sintered microsphere scaffolds. The potential of ADSCs to release angiogenic growth factors is one aspect of this contribution that is potentially applicable to bioengineering of blood vessels into biomaterials for treatment of other tissues. At the same time, the possibility of cotransfection using multiple vectors to mediate the simultaneous production of two or more transgenic proteins is also an advantage of the combined gene therapy–cell transplantation strategy. Another aspect of this study is the higher efficiency of the gene therapy strategy by including the use of tissue-specific cell types. This suggests that an attractive future research direction might be to understand how single-cell behavior translates to tissue organization in multicellular settings.

Materials and Methods

Preparation of the Sintered Microsphere Scaffolds. A 1:4 wt/vol polymer solution was prepared by dissolving PLAGA (85:15 lactide:glycolide ratio, molecular mass = 120 kDa) (Alkermes) in methylene chloride (Fisher Scientific). The polymer solution was added into a 1% poly(vinyl alcohol) (Sigma–Aldrich) solution. The PLAGA/PVA emulsion was stirred for 24 h. The microspheres were isolated by vacuum filtration, washed with deionized water, air-dried for 24 h, and then lyophilized for an additional 24 h to ensure complete solvent removal. Microspheres with size range of 500–710 μm were isolated by using a stainless steel sieve. Porous 3D disk scaffolds (10-mm diameter $\times$ 4-mm thickness) were fabricated by transferring microspheres into a stainless steel mold, which was heated at 80°C for 1.5 h.

ADSC Isolation and Culture. Human adipose tissue was isolated under the approval and guidelines established by the University of Virginia's Institutional Review Board. Briefly, infrapatellar fat tissue was removed and transferred to a sterile dish. The adipose tissue was washed with Krebs–Ringer bicarbonate (KRB; Sigma) to remove blood. Next, the tissue was digested by using a collagenase type I solution (1 g of collagenase per liter of KRB supplemented with 1% BSA) for 60 min at 37°C. DMEM supplemented by 10% FBS was used to neutralize the enzyme activity. The stromal cells were centrifuged for 10 min, and the cell pellet was resuspended in medium (EGM-2MV Bulletkit) (Cambrex$_2$, cells were washed with PBS to remove residual red blood cells.

Adenoviral Transfection of ADSCs. The recombinant adenovirus with human VEGF cDNA was a generous gift from the Meenhard Herlyn laboratory at Wistar Institute (Philadelphia). The adenovirus was constructed by using cotransfection of 293 cells, a cell hyperproduction system, to construct adenovirus as described in ref. 41. Confluent ADSCs at passage 4 were counted and transfected with VEGF containing adenovirus at different MOIs. After a 24-h incubation, the virus-containing culture medium was removed and the cells were washed with PBS three times.

Cell Seeding. Scaffolds were sterilized by immersion in 70% ethanol for 10 min, rinsed with de-ionized (DI) water, and exposed to UV light for 30 min on each side. Next, they were placed into 24-well tissue culture plates and seeded with cells (ADSCs, ECs, or ADSCs+EC). Cells were allowed to attach to scaffolds for 1 h before addition of 2 ml of medium (EGM-2MV Bulletkit) into each well. Cells were maintained in a humidified incubator at 37°C with 5% CO_2.

SEM. The morphology of ADSCs cultured on the scaffolds was assessed at predetermined time points by using SEM. Briefly, cells were fixed at room temperature in 1% and 3% gluteraldehyde for 1 h and 24 h, respectively. The scaffolds were then dehydrated sequentially by using an ethanol series (50%, 70%, 80%, 90%, 95%, and 100%) for 10 min each. Scaffolds were allowed to dry overnight, sputter-coated with gold/palladium, and viewed under SEM (JEOL 6700).

Blood vessel morphology in the scaffolds implanted in mice was also evaluated by using SEM. At 21 days after implantation, scaffolds were cut in half horizontally, fixed with formalin, dehydrated as mentioned above, and sputter-coated with gold/palladium. The SEM images were acquired on each internal side of the scaffolds.

VEGF Production Analysis. ADSCs were seeded at a density of 100,000 per well in a 24-well plate with EGM-2MV media for 24 h. Next, cells were transfected with 2 ml of adenovirus encoding VEGF (Ad-VEGF) solution (Ad-VEGF in media) at MOIs of 0, 5, 10, 20, 50, and 100 for 24 h, after which cells were washed three times with PBS and supplied with fresh media. At days 3, 7, and 10 the media were collected and examined for the level of VEGF by using ELISA (R & D Systems).

Coculture Study. We used coculture six-well plates (0.4-μm pore size) (Corning Life Sciences) to evaluate the mitogenic effect of ADSCs on ECs and the bioactivity

of the VEGF released by transfected ADSCs. Briefly, ADSCs were transfected at MOI = 100 for 24 h in a tissue culture flask. Next, the transfected ADSCs were trypsinized and then centrifuged for 10 min after which the cell pellet was resuspended in medium. Transfected ADSCs at a density of 100,000 cells per plate were cultured at the insert layer of a coculture plate containing ECs at a density of 100,000 cells per plate at the bottom layer. At predetermined time points, the insert layer was removed and the proliferation of ECs was compared with ECs cocultured with ADSCs or cultured alone. To measure the EC proliferation a 3-(4,5-dimethyliazol-2-yl)-5-(3-carboxymethoxyphenyl)-2-(4-sulfophenyl)-2H tetrazolium colorimetric assay (CellTiter 96 AQ_{ueous}; Promega) was used.

Immunofluorescent Analysis of VEGF Production. Transfected ADSCs growing on scaffolds were rinsed with PBS and fixed with 4% paraformaldehyde for 15 min at room temperature. After four washes with PBS, cells were permeabilized with 0.5% Triton X-100 for 10 min. Cells were washed four times with PBS, and 1% BSA (Sigma–Aldrich) in PBS was applied for 30 min at room temperature as a blocking solution. After one wash with PBS, VEGF antibody (1:200 dilution; R & D Systems) was added and incubated overnight at 4°C. The scaffolds were then washed four times with PBS, the secondary antibody (1:800, anti-mouse Alexa Fluor 488; Molecular Probes) was added, and the scaffolds were incubated for 1 h at room temperature. After one wash with PBS, scaffolds were placed in antifade reagent (Molecular Probes) and examined with a confocal laser scanning microscope. Three-dimensional images were created by an assembly of 2D sections of the scaffolds moving through its thickness at depth increments of 4 μm to a focus depth of 224 μm.

***In Vivo* Biomaterial Vascularization Studies.** The *in vivo* experiments were performed with approval and according to the University of Virginia Animal Care and Use Committee. Matrices (n = 5) were implanted (one implantation per animal) s.c. on the dorsal region of 100 6- to 8-week-old male SCID mice. Matrices were treated to minimize bacterial contamination using 70% ethanol followed by a series of rinses with DI water and exposure to UV light on each side for 30 min. For conditions including cell transplantation, cells of each type at a density of 100,000 cells per scaffold were seeded 24 h before implantation. For gene therapy conditions, ADSCs were transfected at MOI = 100 PFU per cell for 24 h, after which they were washed three times with PBS, trypsinized, and seeded on the scaffolds at a density of 100,000 cells per scaffold 24 h before implantation. SCID mice were anesthetized with inhalational methoxyflurane, prepped, and draped. The following six experimental groups were studied: (*i*) 3D PLAGA scaffold (negative control) (blank), (*ii*) scaffold plus ECs (EC), (*iii*) scaffold plus ADSCs (ADSC), (*iv*) scaffold plus ADSCs and ECs (ADSC+EC), (*v*) scaffold plus transfected ADSCs (T ADSC), and (*vi*) scaffold plus transfected ADSCs and ECs (T ADSC+EC). At days 7, 14, and 21, the mice were killed and the scaffolds were retrieved, fixed in formalin, paraffin-embedded, sectioned for histology, and stained with H&E. The number of blood vessels in the pore areas (minimum of 10 randomly selected fields) of the scaffolds (total scaffold surface area $\approx$ 78.5 mm^2, porosity = 31%) was determined by using the images of H&E-stained slides. Sections were visualized by using a Nikon Eclipse E600 epifluorescence microscope at $\times$10 and $\times$100 magnification and analyzed with NIH Image J software. Results are reported in the form of vascular density (number of blood vessels per scaffold)

Statistical Analysis. Five scaffolds were analyzed per condition. Data in graphs represent mean and SD. Statistical significance was calculated by using multiway ANOVA. Comparison between the two means was determined by using the Tukey test, and statistical significance was defined as $P \leq 0.05$.

ACKNOWLEDGMENTS. We thank Dr. Meenhard Herlen for providing the adenovirus with cDNA encoding VEGF. We also thank Dr. Steven P. Wrenn (Department of Chemical and Biological Engineering, Drexel University, Philadelphia) for helping us with the microscopy facility. We are grateful to Dr. Cameron F. Abrams (Department of Chemical and Biological Engineering, Drexel University), Dr. Xudong Li (Department of Orthopaedic Surgery, University of Virginia), and Dr. Brett R. Blackman (Department of Biomedical Engineering, University of Virginia) for helpful discussions. We gratefully acknowledge support from the National Institutes of Health (Grant NIH-RO1-ARO52536).

1. Laurencin CT, Ambrosio AMA, Borden MD, Cooper JA (1990) Tissue engineering: Orthopedic applications. *Annu Rev Biomed Eng* 1:19–46.
2. Burg KJL, Porter S, Kellam JF (2000) Biomaterial developments for bone tissue engineering. *Biomaterials* 21:2347–2359.
3. Langer R, Vacanti JP (1993) Tissue engineering. *Science* 260:920–926.
4. Patel ZS, Mikos AG (2004) Angiogenesis with biomaterial-based drug- and cell- delivery systems. *J Biomater Sci Polymer Edn* 15:701–726.
5. Sharkawy AA, Kiltzman B, Truskey GA, Reichert WM (1998) Engineering the tissue which encapsulates subcutaneous implants. III. Effective tissue response times. *J Biomed Mater Res* 40:598–605.
6. Kidd KR, Nagle RB, Williams SK (2002) Angiogenesis and neovascularization associated with extracellular matrix-modified porous implants. *J Biomed Mater Res* 59:366–377.
7. Freshney RI (1994) *Culture of Animal Cells: A Manual of Basic Techniques* (Wiley, New York).
8. Colton CK (1995) Implantable biohybrid artificial organs. *Cell Transplant* 4:415–436.
9. Tabata Y, Miyao M, Yamamoto M, Ikada Y (1999) Vascularization into a porous sponge by sustained release of basic fibroblast growth factor. *J Biomater Sci Polymer Edn* 10:957–968.
10. Sheridan MH, Shea LD, Peters MC, Mooney DJ (2000) Bioadsorbable polymer scaffolds for tissue engineering capable of sustained growth factor delivery. *J Controlled Release* 64:91–102.
11. Perets A, *et al.* (2003) Enhancing the vascularization of three-dimensional porous scaffolds by incorporating controlled release basic fibroblast growth factors microspheres. *J Biomed Mater Res* 65:489–497.
12. Holder WD, *et al.* (1997) Increased vascularization and heterogeneity of vascular structures occurring in polyglycolide matrices containing aortic endothelial cells implanted in the rat. *Tissue Eng* 3:149–160.
13. Rafii S, Lyden D (2003) Therapeutic stem and progenitor cells transplantation for organ vascularization and regeneration. *Nat Med* 9:702–712.
14. Rosilio V, Benoit JP, Deyme M, Thies C, Madelmont GA (1991) A physicochemical study of the morphology of progesterone-loaded microspheres fabricated from poly(D,L-lactide-co-glycolide). *J Biomed Mater Res* 25:667–682.
15. Young LS, Searle PF, Onion D, Mautner V (2006) Viral gene therapy strategies: From basic science to clinical application. *J Pathol* 208:299–318.
16. Gardlik R, *et al.* (2005) Vectors and delivery systems in gene therapy. *Med Sci Monit* 11:RA110–RA121.
17. Schreiber RE, *et al.* (2005) Bone induction by AdBMP-2/collagen implants. *J Bone Joint Surg Am* 5:1059–1068.
18. Peterson B, *et al.* (2005) Healing of critically sized femoral defects, using genetically modified mesenchymal stem cells from human adipose tissue. *Tissue Eng* 11:120–129.
19. Ohno N, *et al.* (2002) Accelerated reendothelialization with suppressed thrombogenic property and neointimal hyperplasia of rabbit jugular vein grafts by adenovirus-mediated gene transfer of C-type natriuretic peptide. *Circulation* 105:1623–1626.
20. Fields RC, Solan A, McDongah KT, Niklason LE, Lawson JH (2003) Gene therapy in tissue-engineered blood vessels. *Tissue Eng* 9:1281–1287.
21. Kurozumi K, *et al.* (2004) BDNF gene-modified mesenchymal stem cells promote functional recovery and reduce infarct size in the rat middle cerebral artery occlusion model. *Mol Ther* 9:189–197.
22. Iwaguro H, *et al.* (2002) Endothelial progenitor cell vascular endothelial growth factor gene transfer for vascular regeneration. *Circulation* 105:732–738.
23. Caterson EJ, Nesti LJ, Danielson KG, Tuan RS (2002) Human marrow-derived mesenchymal progenitor cells—Isolation, culture expansion, and analysis of differentiation. *Mol Biotechnol* 20:245–256.
24. Zuk PA, *et al.* (2001) Multilineage cells from human adipose tissue: Implications for cell-based therapies. *Tissue Eng* 7:211–228.
25. Halvorsen YC, Wilkison WO, Gimble JM (2000) Adipose-derived stromal cells—Their utility and potential in bone formation. *Int J Obes Relat Metab Disorders Suppl* 4:S41–S44.
26. Planat-Benhard V, *et al.* (2004) Plasticity of human adipose lineage cells toward endothelial cells—Physiological and therapeutic perspectives. *Circulation* 109:656–663.
27. Cao Y, *et al.* (2005) Human adipose tissue-derived stem cells differentiate into endothelial cells in vitro and improve postnatal neovascularization in vivo. *Biochem Biophys Res Commun* 332:370–279.
28. Rehman J, *et al.* (2004) Secretion of angiogenic and antiapoptotic factors by human adipose stromal cells. *Circulation* 109:1292–1298.
29. Nakagami H, Maeda K, Kaneda Y, Ogihara T, Morishita R (2005) Novel autologous cell therapy in ischemic limb disease through growth factors secretion by cultured adipose tissue-derived stromal cells. *Arterioscler Thromb Vasc* 25:2542–2547.
30. Borden M, Attawia M, Khan Y, El-Amin SF, Laurencin CT (2004) Tissue-engineered bone formation in vivo using a novel sintered polymeric microsphere matrix. *J Bone Joint Surg* 86B:1200–1208.
31. Jabbarzadeh E, Jiang T, Nair LS, Khan YM, CT Laurencin. (2007) Human endothelial cell growth and phenotypic expression on three dimensional poly(lactide-co-glycolide) sintered microsphere scaffolds for bone tissue engineering. *Biotechnol Bioeng* 98:1094–1102.
32. Folkman J, Klagsburn (1987) Angiogenic factors. *Science* 235:442–447.
33. Jiang T, Abdel-Fattah WI, Laurencin CT (2006) In vitro evaluation of chitosan/poly(lactide acid-glycolic acid) sintered microsphere scaffolds for bone tissue engineering. *Biomaterials* 27:4894–4903.
34. Koransky ML, Robbins RC, Blau HM (2002) VEGF gene delivery for treatment of ischemic cardiovascular disease. *Trends Cardiovasc Med* 12:108–114.
35. Verma IM, Somia N (1997) Gene therapy—Promises, problems and prospects. *Nature* 389:239–242.
36. Kafri T, *et al.* (1998) Cellular immune response to adenoviral vectors infected cells does not require *de novo* viral gene expression: Implications for gene therapy. *Proc Natl Acad Sci USA* 95:11377–11382.
37. Benihoud K, *et al.* (2007) Respective roles of TNF-alpha and IL-6 in the immune response elicited by adenovirus-mediated gene transfer in mice. *Gene Ther* 14:533–544.
38. Robbins PD, Ghivizzani SC (1998) Viral vectors for gene therapy. *Pharmacol Ther* 80:35–47.
39. Kang SK, Jun ES, Bae YC, Jung JS (2003) Interactions between human adipose stromal cells and mouse neural stem cells in vitro. *Dev Brain Res* 145:141–149.
40. Elbjeirami WM, West JL (2006) Angiogenesis-like activity of endothelial cells cocultured with VEGF-producing smooth muscle cells. *Tissue Eng* 12:381–390.
41. Gruss CJ, *et al.* (2003) Stroma formation and angiogenesis by overexpression of growth factors, cytokines, and proteolytic enzymes in human skin grafted to SCID mice. *J Invest Dermatol* 120:683–692.